EUROPEAN CONFERENCE ON INTEGRATED OPTICS

Towards on-chip wavelength modulation spectroscopy at 1.5 µm via InP integrated photonics and low-cost driving hardware

(Conference paper)

Stefano Tondini[1], Jun Zhang[2], Joel Hazan[1], Martijn Heck[1] and Jia Chen[2]

[1]Eindhoven Hendrik Casimir Institute, Eindhoven University of Technology, Eindhoven, 5612 AE, Netherlands
[2]Environmental Sensing and Modeling, Technische Universität München, Munich, 80333, Germany
* s.tondini@tue.nl

Photonics allows for unprecedented miniaturization and speeding-up of many technological concepts. The case here presented consists of a compact gas-sensing system based on a single photonic integrated circuit with a tunable laser and a photodetector realized on InP and wavelength modulation spectroscopy. Looking out towards the exploitation of such a concept in the field, the feasibility of implementing all the driving and signal processing tasks on a low-cost microcomputer is verified.
Keywords: *Integrated tunable laser, indium phosphide photonic integration, pollution sensing, absorption spectroscopy, digital lock-in amplifier.*

INTRODUCTION

This work aims at prompting the gas sensing performances that can be achieved on a photonic chip by means of a wavelength modulation spectroscopy (WMS) scheme implemented through low-cost hardware. On the one hand, a photonic integrated circuit encompassing a tunable laser with a 50 nm range centered at 1.5 µm and a high-responsivity photodetector can be conveniently realized in the mature InP technology [1] to be coupled with a hollow-core fibre serving as a gas interaction cell [2,3]. On the other hand, advanced absorption spectroscopy techniques can be synthesized on a single microcontroller unit (e.g. Raspberry Pi), which acts as both a laser driver and a digital lock-in amplifier [4] for the signal-to-noise ratio (SNR) improvement of the gas detection. This preliminary study carries the high-level description of a compact system with multi-species pollutant sensing capabilities, detailed for the example of ammonia (1512 nm). The capacity of the system to potentially target different pollutant gases, i.e. N_2O and CH_4, at the same time is ensured by the wide laser tunability range.

SYSTEM/EXPERIMENT DESIGN

The sensing system architecture is depicted in Fig. 1., where three main building blocks can be identified, namely the driving control unit (green rectangle on the left), the photonic integrated circuit (grey square in the middle), and the gas interaction cell that is represented on the right by a coiled hollow-core fibre. It is worth mentioning that, due to the limited sampling and processing frequency required by the WMS (generally, about a few kHz), a digital lock-in amplifier to serve the spectroscopy purpose can be achieved on a low-cost microcomputer. Two main tasks have to be implemented on that. The first is a particular laser driving scheme, which is going to be detailed in the next section. The second is the digital signal processing, described in the Outlook section, to decrease the 1/f noise and increase the SNR.

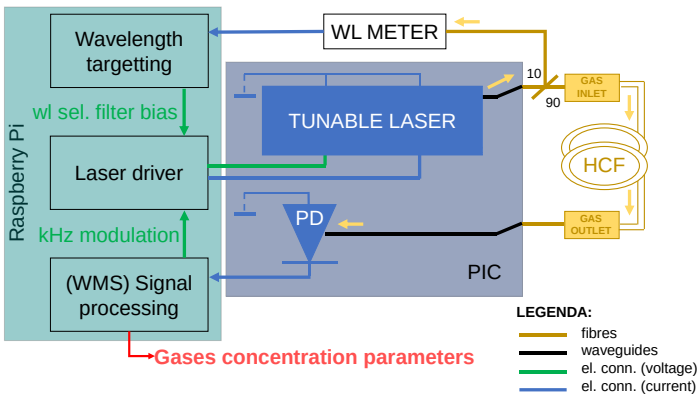

Fig. 1. Schematics of the sensing system where a single microcontroller unit is managing the wavelength targeting, the laser driving and the digital lock-in amplifier tasks on the left, a photonic integrated chip embeds both the light source and the photodetector in the middle, and a hollow-core fibre serves as gas interaction cell on the rightmost part.

Another fundamental task to accomplish is the optical feedback on the laser output, to perform periodical checks/calibrations against drifting and therefore to maintain a box-shaped laser emission all along with the tuning range. This can be achieved by means of a Fiber Bragg Grating metrology system [5] through splitting the laser output.

WMS DRIVING SCHEME

When performing gas spectroscopy in a noisy environment, which is a common condition for air pollution measurements, the wavelength modulation technique allows for extracting only the signal component at the desired frequency and phase, filtering out the other noise contributions [6]. In this section, the driving scheme to apply to the tunable laser is described, based on previous experiments carried out with a commercial laser source [4]. Fig. 2. (a) shows the wavelength modulation as the summation of a slow saw-tooth function and a fast but with smaller amplitude sinusoidal function. With our special laser design (Fig. 2 (c)), we can address the saw-tooth scanning and the sinusoidal oscillation through two separate laser sections. Indeed, inside the Fabry-Perot cavity (Fig. 2 (d)), besides a semiconductor optical amplifier (SOA) we find a 8-arms folded Mach-Zehnder Interferometer (MZI) with linearly increasing imbalances as an intra-cavity wavelength selection filter and an in-line Electro-Optical Phase Modulator (EOPM) for adjusting the cavity modes. Even though the effect of tuning the intra-cavity filter and the in-line EOPM mutually affect each other, we can assume they are independent by involving a compensation term in the filter driving. Therefore, for the low scanning component, we can slide the filter pass-band back and forth on a target wavelength range, and we can fast modulate the wavelength by trimming on the cavity modes (Fig. 2. (b)). The modulation frequency is accomplished by reversely biasing the EOPMs deployed on the MZI arms, capable of up to GHz bandwidth. Some relevant design figures are: 4mm FP cavity length, 800 µm SOA length, 1MHz laser expected linewidth, and a 0.16 nm FP cavity mode spacing. Output optical power in the range of mWs on-chip and 0.85 A/W responsivity photodetectors performances are expected out of the mature InP fabrication platform. Worth to notice is that the 3nm scanning window of Fig. 2. (a) has been selected to match the ammonia absorption peak that is going to be taken as an example in the following section. However, this range can be extended more than 10 times, to target, at the same time, other gas species, which have marked absorption peaks around 1.5 µm.

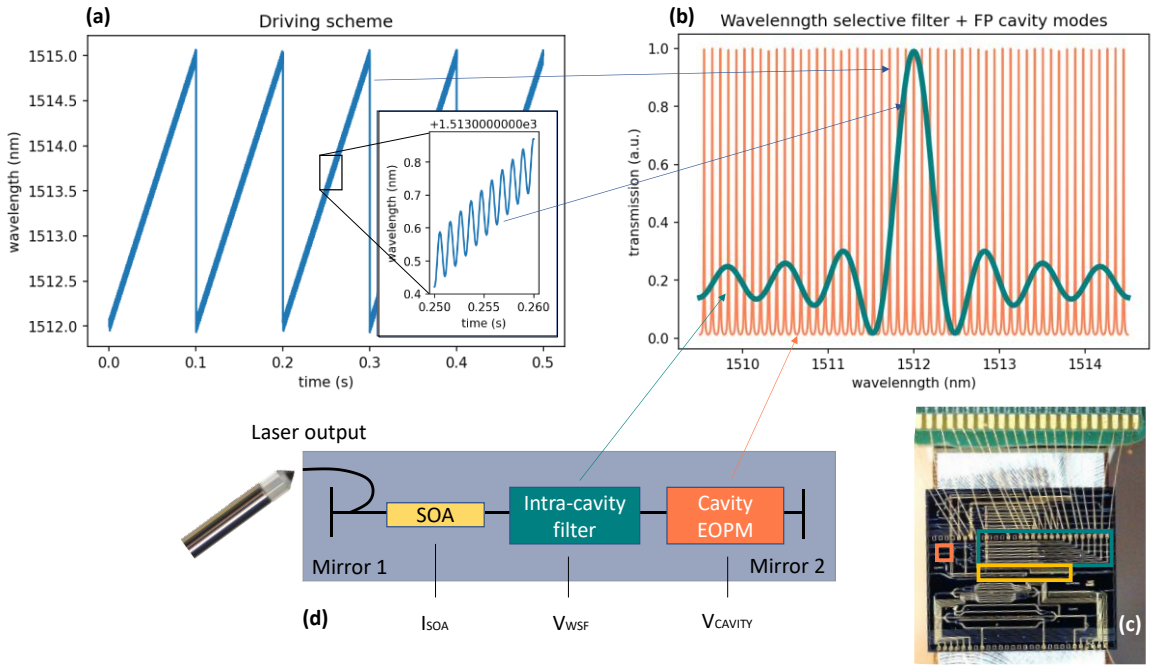

Fig. 2. (a) Ideal driving scheme to be applied to the laser source to achieve WMS, where a slow linear scan over 3 nm is performed at 10 Hz and a faster and smaller sinusoidal modulation at 6 kHz is superimposed to decrease the 1/f noise and to increase the SNR. (b) Simulation of the intra-cavity wavelength selective filter, in green, and the longitudinal modes of the laser cavity, in orange. By the laser design (c-d), these figures can be independently tuned and then the slow and the fast components of the driving scheme can be decoupled, leading to easier laser management during the WMS.

PRELIMINARY FIGURES

As a preliminary result, we show the laser output range in a contour plot, Fig. 3 (a). The map has been built sequentially, by collecting the output spectrum with an optical spectrum analyzer for 1000 target wavelength steps

from the bottom value of 1510 nm to the top value of 1560 nm. It is notorious that the main optical signal lies on the diagonal. This confirms the tuning algorithm applied is well-suited to predict the laser behaviour. The laser output map can be scrubbed from the spurious wavelengths of the multi-mode configurations by means of a dedicated fine-tuning algorithm. However, this is a challenging operation as such noise is mainly due to temperature and humidity variation at the photonic chip level. Alongside the laser figures, Fig. 3. (b) carries a simulation of the NH_3, CO_2, and H_2O absorption lines around 1512 nm at atmospheric conditions (P = 0.96 atm, T = 296 K) for a 30 m optical path length. The plot is based on HITRAN data [7]. While H_2O and CO_2 concentrations are set to realistic average outdoor values, NH_3 is encompassed in the simulation with a 10 ppm concentration. The reason is to show that we can get to a 2% absorbance in such conditions, being not hindered by water vapour and carbon dioxide interferences [8]. Considering a typical absorbance resolution of a WMS system to be 10^{-5}, a detection limit of 5 ppb for NH3 can be achieved [9,10].

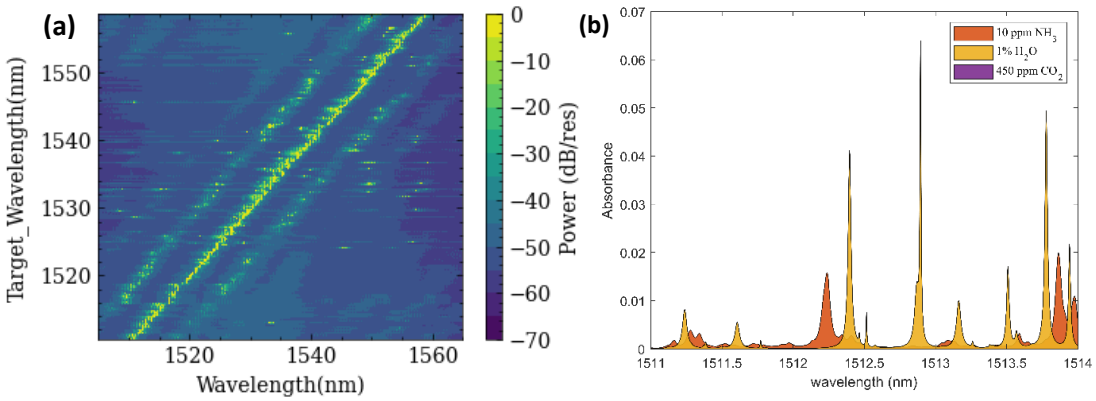

Fig. 3. (a) Tunable laser emission range where the single output wavelengths are emitted sequentially as a deterministic control strategy can be applied to target a specific emission condition. The side modes, which are visible from the contour can be further suppressed by operating the fine-tuning stage of the intra-cavity filter. (b) HITRAN Simulations of the H_2O, CO_2, and NH_3 absorption lines around 1512 nm under atmospheric conditions (P = 0.96 atm, T = 296 K) with a 30 m interaction path length.

OUTLOOK

Advanced WMS techniques can be applied to go beyond the limits of detection recently estimated for 1.5 µm photonics integrated circuits in levels of 100 ppb for NH_3 and at ppm for NO_2 (when considering common noise figures of multi project wafers) [6]. Multi-harmonic based WMS will further allow for improving sensor sensitivity, detection precision and SNR, especially in a harsh environment [3] (real-operation condition). This concept will be experimentally proven in upcoming works.

Acknowledgements: this project has received funding from European Union's Horizon 2020 programme under GA no. 899987.

References

[1] L. M. Agustin, et al., *InP-Based Generic Foundry Platform for Photonic Integrated Circuits*, IEEE Journal of Selected Topics in quantum electronics, vol.24, no. 1 2018
[2] A. Hänsel, M. Heck, *Opportunities for photonic integrated circuits in optical gas sensors*, J. Phys.: Photonics, vol. 2, 2020
[3] J. Chen, et. al., *Low-level and ultralow-volume hollow waveguide based carbon monoxide sensor*, Optics Letters, vol. 45, no. 21, pp. 3577-3579, 2010
[4] Lan, L. et al., *Self-Calibrated Multiharmonic CO2 Sensor Using VCSEL for Urban In Situ Measurement*, IEEE Transactions on Instrumentation and Measurement, vol. 68, 2019
[5] M. Muneeb, et al., Silicon-on-insulator shortwave infrared wavelength meter with integrated photodiodes for on-chip laser monitoring, Optics Express, vol. 22, no. 22, pp 27300-27308, 2014
[6] A. Hänsel, M. Heck, *Feasibility of Telecom-Wavelength Photonic Integrated Circuits for Gas Sensors*, Sensors vol. 18, no. 9, 2018
[7] https://hitran.org/
[8] Ligang Shao, et al., *Simultaneous detection of atmospheric CO and CH4 based on TDLAS using a single 2.3 µm DFB laser*, Spectrochimica Acta Part A: Molecular and Biomolecular Spectroscopy, vol. 222, no. 5, 2019
[9] J. Chen, et. al., *VCSEL-based calibration-free carbon monoxide sensor at 2.3 µm with in-line reference cell*, Applied Physics B, no. 102, pp 381–389, 2011
[10] J. Chen, et. al., *Laser spectroscopic oxygen sensor using diffuse reflector based optical cell and advanced signal processing*, Applied Physics B, no. 100, pp 417–425, 2010